PAPER

Check for updates

Synthesis of size-controlled and highly monodispersed silica nanoparticles using a short alkyl-chain fluorinated surfactant†

Saravanan Nagappan,[a] Anandhu Mohan,[a] Anju Maria Thomas,[a] Jong-Man Yoo,[a] Nadim Eid,[b] Ildoo Chung, [ID][a] Bruno Ameduri [ID][b] and Chang-Sik Ha [ID] *[a]

Highly monodispersed silica nanoparticles (SiNPs) were synthesised using a fluorinated surfactant, $HOCH_2CH(CF_3)CO_2H$, and its efficiency was compared with efficiencies of five other surfactants. The size of the SiNPs ($\sim$50–200 nm) was controlled by controlling the surfactant amount. The short alkyl-chain fluoro surfactant was found to be more efficient at producing monodispersed SiNPs than its long alkyl-chain fluoro or non-fluorinated surfactant counterparts.

Introduction

Recently, silica nanoparticles (SiNPs) have attracted considerable attention in various applications such as drug delivery; adsorption and separation of proteins, dyes, metal ions, and oil/water; and catalysis, among others.[1–7] The main advantages of using SiNPs are their low toxicity, excellent thermal stability, facile approach, biocompatibility, abundance in earth, and easier synthesis.[1,8] Another advantage of SiNPs is their ability to modify surface properties with various functional groups for developing hydrophilic and hydrophobic functional groups, which may enhance the dispersibility, stability, and compatibility with other materials.[9–11] SiNPs are widely utilised as fillers or supporting materials.[12,13] Sol–gel techniques, templating, colloidal, hydro-thermal, and solvo-thermal methods are applied widely for the synthesis of monodispersed and narrow size distribution of SiNPs.[12,14–17] The hydroxylation and condensation of alkoxy silane precursors can facilitate development of SiNPs with an amorphous network of silicon and oxygen groups.[18] SiNPs synthesised with mesoporous and nanoporous structures have also garnered interest in various fields due to their high surface area, pore volume, and pore diameter with highly controlled porosity, and their ability to adsorb large quantities of drugs, dyes, metal ions, and organic compounds.[12,19,20] The uniform particle size, shape,

morphology, and control of aggregation behaviours of the synthesised SiNPs are important parameters for various applications because particles with larger sizes or uneven morphologies may limit the practicality of SiNPs for some applications. Therefore, controlling these properties is essential. The above properties of synthesised SiNPs must be controlled by selecting and optimising experimental conditions, such as a proper silane precursor, surfactant, rotation speed, reaction time, temperature, water, and catalyst.[14,21–23]

A surfactant (*i.e.*, surface active agent) plays a crucial role in stabilising and controlling the shape and morphology of synthesised particles, because a surfactant usually acts as a template to form micelles as well as a stabilising agent for developing uniform NPs.[24,25] Nevertheless, a surfactant is expensive, which is a major drawback limiting its usage for bulk synthesis.[26] The controlled particle size and shape are quite important for several applications, especially biomedical.[12,27] Various surfactants are used to synthesise porous or non-porous SiNPs, such as cetyltrimethylammonium bromide (CTAB) and cetyltrimethylammonium chloride (CTAC).[12] The effect of surfactants on the synthesis of porous SiNPs has been studied by several researchers because of the diverse applications of porous SiNPs.[12] Non-porous SiNPs have also been studied for various applications. The continuous need for monodispersed SiNPs for various applications is of great interest to develop using different methods.

In recent years, a considerable amounts of research has been carried out on the synthesis of uniform SiNPs by using the conventional Stöber method because of its excellent applicability in various applications such as adsorption of heavy metals and proteins, separation of organic compound, drug delivery, coating, and so on. For instance, Murray *et al.* synthesised a highly monodispersed spherical SiNPs by the Stöber method in three pathways of synthesis.[28] In the first case, they synthesised SiNPs with diameters of 15–25 nm by the hydrolysis of

[a]Department of Polymer Science and Engineering, Pusan National University, Busan, 46241, Republic of Korea. E-mail: csha@pnu.edu

[b]Institute Charles Gerhardt, CNRS, University of Montpellier, ENSCM, Montpellier, France

† Electronic supplementary information (ESI) available: FESEM and FETEM images, FTIR spectra with some discussions, XRD patterns, TGA thermograms, degradation behaviour of MAF-OH, nitrogen adsorption and desorption isotherms of the SiNPs prepared at various conditions, and table of textural properties, zeta potentials, average particle size values of samples prepared in the presence of various surfactants, BC and AC. See DOI: 10.1039/d0ra08114k

tetraethyl orthosilicate (TEOS) in aqueous ammonia in ethanol, followed by further reaction with octadecyltrimethoxysilane (ODTMS). In the second route, one-pot synthesis of SiNPs with diameters of 15–50 nm was achieved by the hydrolysis of TEOS in amino acid, followed by being coated with ODTMS. In the third pathway, direct hydrolysis of ODTMS in aqueous ammonia-ethanol solvents also lead to highly monodispersed SiNPs with diameters of 15–30 nm. Tadanaga *et al.* also synthesised spherical SiNPs with sizes less than or above 10 nm with some aggregation of SiNPs by the Stöber method with high concentration of TEOS in the presence of aqueous ammonia and ethanol.[14] The size of different SiNPs was controlled by varying the TEOS/ethanol molar ratio. Rahman *et al.* reviewed various synthesis pathways of uniform SiNPs by the sol–gel method and their applications in silica-polymer nanocomposites.[15]

Kim *et al.* also carried out a synthesis of size controlled spherical SiNPs by hydrolysis and condensation of silane precursor by the Stöber sol–gel method.[23] The reaction was performed by dissolving TEOS precursor in water and ethanol, followed by the addition of ammonia solution. The size of SiNPs can be tuned from 30–300 nm by adjusting the water/ammonia ratio and the rotation speed with optimised amount of ethanol. Quan *et al.* also synthesised a uniform and highly monodispersed SiNPs by the Stöber method with the size ranging from 7 to 4100 nm using alkaline buffer solution, by altering various reaction parameters such as temperature and different alkaline buffer, and with doping with fluorescent dye.[29] Han *et al.* reported the growth mechanism of SiNPs by the Stöber method using TEOS, ethanol, water, and ammonia solution, and produced spherical SiNPs (15–230 nm).[30] Recently, Ren *et al.* studied the combined micro-channel and microwave method for the synthesis of uniform spherical SiNPs because the combined method can help to process the nucleation and growth of SiNPs in basic medium and provide the uniform particles size in the range from 15 to 400 nm.[31]

In this study, various types of surfactants were tested, such as non-halogenated surfactants with different chain lengths (heptanoic acid (HA, $C_6H_{13}CO_2H$) and nonanoic acid (NA, $C_8H_{17}CO_2H$)) and fluorinated (perfluoropentanoic acid (PFPA, $C_4F_9CO_2H$) and perfluorohexanoic acid (PFHA, $C_5F_{11}CO_2H$)) surfactants with carboxylic functional end-groups for the size-controlled synthesis of monodispersed SiNPs (Scheme 1). Each surfactant concentration was fixed at 0.5 mmol with constant amounts of water, ethanol, ammonia, and silane precursor. 3-Hydroxy-2-(trifluoromethyl)-propanoic acid (MAF-OH, $C_3H_4F_3OCO_2H$) is a degradable difunctional fluorinated surfactant with hydrophilic carboxylic acid and hydroxyl functions and a hydrophobic fluorinated group. The MAF-OH surfactant has been used in various applications.[32–34] MAF-OH was introduced for the first time to synthesise SiNPs. The addition of a small MAF-OH amount (0.5 mmol) can significantly control the particle size, shape, and morphology of SiNPs compared with those achieved in the absence of such a surfactant. By increasing the MAF-OH amount during SiNPs synthesis, the above characteristics can also be controlled to some extent, while a slight aggregation of particles was
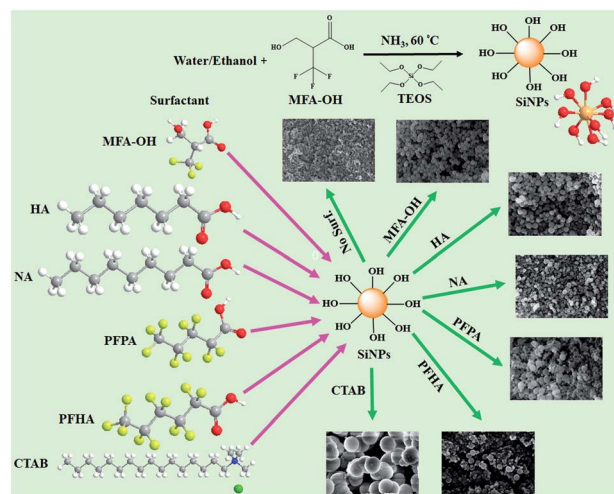
Scheme 1 Synthesis routes of SiNPs and the effect of various surfactants used for the controlled synthesis of SiNPs (note that except TEOS, all acronyms refer to surfactants).

observed at higher MAF-OH concentrations. The novelty of this study is that the use of MAF-OH may significantly tune the particle size, shape, and morphology for the synthesis of uniform, controlled, and monodispersed SiNPs, which broadens the use of NPs for applications such as in fillers, as support for catalysis, in biomedical applications, and coatings. The synthesised SiNPs were analysed using various techniques to characterise the role of MAF-OH in the controlled synthesis of SiNPs (*vide infra*). Scheme 1 illustrates the synthesis pathway of SiNPs using tetraethyl orthosilicate (TEOS) precursor and various surfactants in the presence of a water/ethanol co-solvent and ammonia as the catalyst.

Experimental

Materials

Tetraethyl orthosilicate (TEOS), heptanoic acid (HA), nonanoic acid (NA), perfluoropentanoic acid (PFPA), perfluorohexanoic acid, cetyltrimethylammonium bromide (CTAB), and potassium bromide were purchased from Sigma-Aldrich, Korea. Anhydrous ethanol (reagent grade, 99.9%) was supplied by Samchun Pure Chemical Co. Ltd. Ammonia (NH_3, 28%) was purchased from Junsei Chemical Co., Ltd (Korea). Milli-Q (18 MΩ cm) deionised water was used for all experiments. 2-Trifluoromethacrylic acid (MAF) was kindly supplied by Tosoh Fine Chemicals Corporation (Shunan, Japan).

Synthesis of 3-hydroxy-2-(trifluoromethyl)propanoic acid(MAF-OH)

The synthesis of MAF-OH was performed according to a previously reported procedure.[32–34] MAF (5.0 g, 35 mmol) was dissolved in 500 mL of water and stirred at 74 °C for 26 h. The final solution was lyophilised in a Christ equipment, model Alpha 2-4 LDplus, at −85 °C and 0.88 mbar to allow complete drying for 16 h. After lyophilisation, a whitish wax was obtained.

Synthesis of monodispersed silica nanoparticles (SiNPs) without surfactant

The monodispersed SiNPs were synthesised by mixing 100 mL of water/ethanol (1 : 1) in a 250 mL round-bottom flask followed by the addition of 5 mL of NH_3 solution (28%) and was stirred (500 rpm) in an oil bath at 60 °C for 10 min under nitrogen atmosphere. TEOS (2.08 g, 10 mmol) was added slowly into the solution using a syringe and stirred under a nitrogen atmosphere for 2 h. The transparent solution slowly became light opaque after the addition of TEOS, which indicates the development of SiNPs. The reaction was stopped after 2 h and cooled at 25 °C, the suspension was centrifuged at 15 000 rpm, washed several times in water and ethanol, and dried at 60 °C in an oven followed by vacuum drying at 60 °C for 12 h. The obtained particles showed an average particle size of approximately 45 nm.

Synthesis of monodispersed and uniform SiNPs using MAF-OH surfactant

The same procedure as above was conducted with the same reactants except using MAF-OH (5 mmol). The obtained particles showed an average particle size in the range of 55–90 nm. Similar experimental procedures were repeated with 1.0, 1.5, 2.0, and 2.5 mmol of MAF-OH. A gradual increase in particle size (80–170 nm) was observed as the MAF-OH concentration increased. Surfactants present in the SiNPs were removed by calcination at 540 °C for 8 h at a heating rate of 1 °C min^{-1} to reach the desired temperature and cooled to room temperature after 8 h.

Synthesis of monodispersed SiNPs using HA, NA, PFPA, PFHA, and CTAB surfactants

The synthesis of SiNPs was conducted by following similar reaction conditions with the addition of a fixed concentration of HA, NA, PFPA, PFHA, and CTAB surfactants (0.5 mmol).

Characterisation

The surface morphology and particle shape of the obtained SiNPs were analysed by field emission scanning electron microscopy (FESEM) using SUPRA25 (Carl Zeiss AG, Germany). Prior to measurement, the experiment was performed by uniformly placing the samples on carbon tape, followed by platinum coating. The surface properties were also measured further by field emission transmission electron microscopy (FETEM, Hitachi H-7600, Japan). The FETEM experiment was conducted on a copper grid. Samples were ultrasonically treated in ethanol and loaded on a copper grid, and then gently drying off the solvent using an air dryer. The functional groups available in the SiNPs were identified via Fourier transform infrared spectroscopy (FTIR, JASCO (FTIR-4100), Japan). The SiNPs sample was mixed well with potassium bromide (KBr) and made into a pellet, which was then characterised by FTIR spectroscopy. The FTIR spectra were recorded in the scanning range of 400–4000 cm^{-1}. X-ray diffraction (XRD) was performed using a Miniflex goniometer using Cu Kα irradiation at a scanning

range of 10.0°–80.0° (2θ) with a scanning speed of 0.1° (2θ). The thermal stability of the samples was determined by thermogravimetric analysis (TGA) (TGA Q50 V6.2 Build 187, TA Instruments, USA) at a heating rate of 10 °C min^{-1} under a constant nitrogen flow (100 mL min^{-1}). The nitrogen adsorption–desorption isotherms were used to calculate the surface area and pore volume of the samples at 77 K using Micromeritics ASAP 2020 V3.04 G. The samples were degassed for 12 h under vacuum at 353 K. The specific surface areas were calculated using the Brunauer–Emmet–Teller (BET) method, and pore volumes were determined from the Barrett–Joyner–Halenda (BJH) cumulative desorption pore volume curves. The SiNP surface charge was identified using a Zetasizer Nano S90 (Malvern Instruments Ltd) and calculated from Malvern Zetasizer Software v7.11 PSS0012-37. Samples were prepared by dispersion in deionised water and the average value was obtained by three repeated experiments. The average particle size of the samples was assessed using ImageJ software. Prior to the measurement, the samples were ultrasonicated for 30 min.

Results and discussion

First, the particle shape and surface morphology of the synthesised SiNPs in the absence of surfactant were analysed using FESEM (Fig. 1a). The obtained SiNPs depicted spherical as well as ovoid (egg-like) shapes with a hierarchical surface morphology (Fig. 1a), and the average particle size predicted using ImageJ software was approximately 47 ± 7 nm (Fig. 1a and 2). Moreover, the particle size and shape obtained using this approach were not uniform, and some aggregation was observed due to electrostatic attraction and hydrogen bonding between particles.[24] The FETEM images of the synthesised SiNPs in the absence of surfactant also show similar surface morphologies with average particle size (45–50 nm) (Fig. 2, 3a, and S3, ESI†). It was found that when no surfactant was added, the particle size and shape were not uniform and slight aggregation of SiNPs with hierarchical surface morphology (Fig. 3a, and 4a). This might be due to the inconsistent growth of SiNPs without any surfactant.

The introduction of HA and NA yielded SiNPs with spheres of average size in the ranges of 105 ± 40 and 81 ± 20 nm,
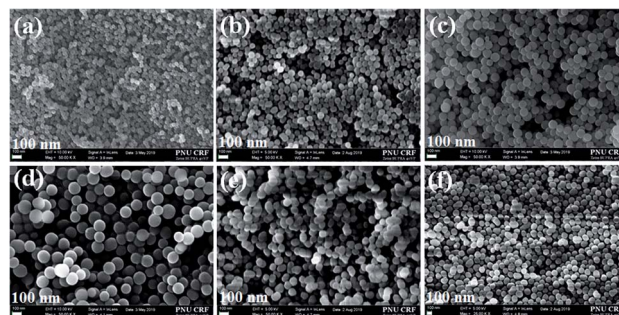

Fig. 1 FESEM images of the synthesised SiNPs (a) in the absence of MAF-OH and (b–f) in the presence of MAF-OH at various concentrations such as 0.5, 1.0, 1.5, 2.0, and 2.5 mmol, respectively, before calcination (BC).
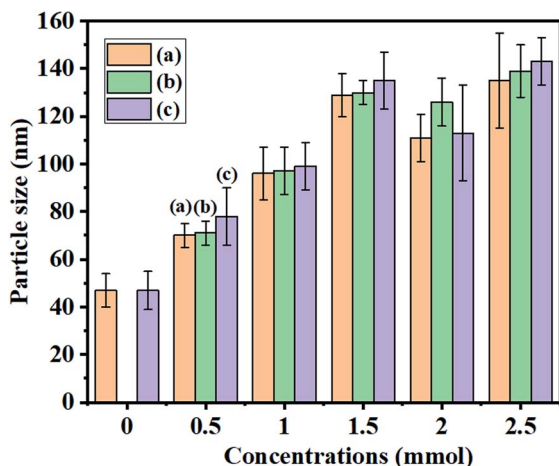
Fig. 2 Particle size histograms of the SiNPs prepared (a) in the absence (0 mmol) and presence of MAF-OH at various concentrations, 0.5, 1.0, 1.5, 2.0, and 2.5 mmol, respectively. The values obtained from FESEM images (a) BC and (b) after calcination (AC); and (c) from FETEM images BC.
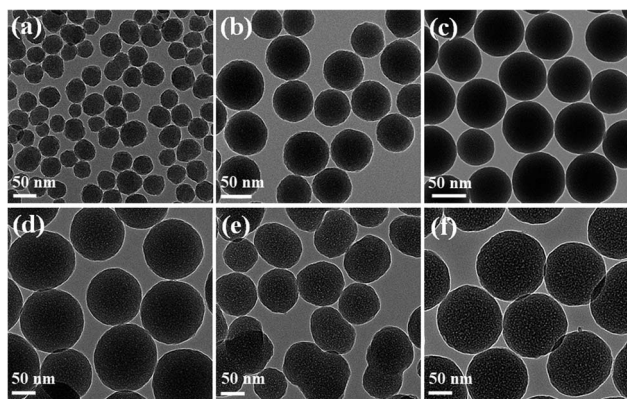

Fig. 3 FETEM images of the synthesised SiNPs at higher magnification (a) in the absence of MAF-OH and (b–f) in the presence of MAF-OH at various concentrations such as 0.5, 1.0, 1.5, 2.0, and 2.5 mmol, respectively, BC.

respectively (Table S1, ESI†). Some non-uniformly aggregated particles with small and large sizes were obtained for both HA and NA (Fig. S1, ESI†). Similarly, more aggregated particles with dual sizes were produced using PFPA (53 ± 12 and 131 ± 8 nm) and PFHA (58 ± 8 and 156 ± 15 nm) surfactants (Fig. S2 and Table S1, ESI†). Similar characterisations were performed for the as-synthesised SiNPs prepared using MAF-OH. The particle shape and surface morphology of the resulting SiNPs at various MAF-OH concentrations are presented in Fig. 1b–f. The SiNPs also showed a uniform spherical shape (Fig. 1 and 3) The hierarchical surface of the SiNPs noted in the absence of MAF-OH was slightly altered when the surfactant was introduced.

Furthermore, studying the relationship between the particle shape and morphology based on the effect of MAF-OH showed that an increase in the MAF-OH concentration yielded more uniform monodispersed SiNPs (Fig. 1b–f and 2). On the other

hand, the average particle size increased (70–150 nm, Table 1) gradually with an increase in the MAF-OH concentration and slight aggregation was observed at higher concentrations (Fig. 1b–f). An average particle size histogram and FETEM images also expressed uniform and monodispersed SiNPs produced by increasing the MAF-OH concentration (Fig. 2, 3b–f, and S3, ESI†).

The abundant availability of carboxylic acid and hydroxyl functional groups in MAF-OH enhances the surface binding of nanoparticles by hydrogen bonding.[35] The weak van der Waals forces of interaction, electrostatic attraction, and hydrogen bonding of MAF-OH at higher concentrations with SiNPs may result in slight affinity between particles, which induces aggregation behaviour.[36,37]

SiNPs synthesised using the MAF-OH surfactant were further calcined at 540 °C, and then, the particle shape and surface morphology of the resulting samples were analysed (Fig. 2 and 4). These calcined samples also demonstrate the formation of highly uniform and monodispersed SiNPs. The histogram obtained from the FESEM and FETEM images (Fig. 2) clearly depicts the role of MAF-OH in controlling the particle size of SiNPs. In summary, it was noted that the introduction of MAF-OH can control the particle uniformity, develop monodispersed SiNPs up to optimum concentrations (up to 1.5 mmol), but cause slight particle aggregation at higher concentrations (Fig. 2, 3b–f, and 4a–e). In particular, the introduction of 0.5 mmol of MAF-OH led to highly uniform and monodispersed spherical SiNPs (70–80 nm) (Fig. 1b and 2).

The surface functionalities, crystal structure, thermal stabilities, surface areas, pore volumes, and pore diameters of the synthesised materials were characterised via FTIR spectroscopy, X-ray diffraction, TGA, and nitrogen adsorption and desorption isotherms. The results obtained are illustrated in Fig. S4–S7 (ESI†). The FTIR spectra of the synthesised SiNPs showed the presence of strong Si–O–Si and Si–OH peaks at 1080, 800, 470, and 950 cm^{-1} in the SiNPs (Fig. S4, ESI†). A small band centred at 1400 cm^{-1} was assigned to the presence of trace amounts of the surfactant. Owing to the high solubility of the surfactant, other peaks were not present because of surfactant leaching from the sample during the washing cycles (Fig. S4, ESI†). From the XRD patterns, all the synthesised SiNPs
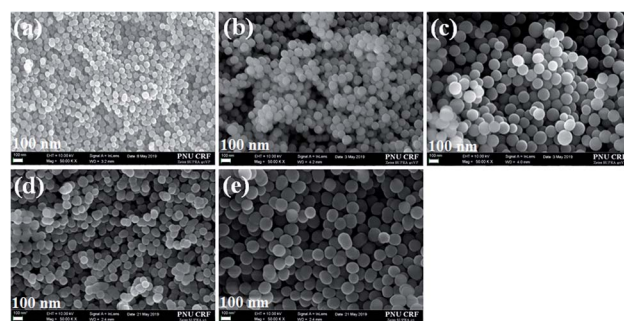

Fig. 4 FESEM images of the SiNPs prepared in the presence of MAF-OH at various concentrations, (a–e) 0.5, 1.0, 1.5, 2.0, and 2.5 mmol, respectively, AC.

Table 1 Surface areas, pore volumes, and pore diameters of samples obtained from the nitrogen adsorption and desorption isotherms, as well as pore-size distribution curves, zeta potential, and average particle size values of samples without surfactant or in the presence of surfactant at various concentrations BC and AC[a]

Sample	BET surface area ($m^2 \, g^{-1}$)	Total pore volume ($cm^3 \, g^{-1}$)	BJH pore diameter (nm)	Zeta potential Value (mV)	Average particle size (nm)
WX	331	0.58	7	−21.6	47 ± 7
$X_{0.5}BC$	244	0.39	7	−23.9	70 ± 5
$X_{1.0}BC$	20	0.17	15	−37.9	96 ± 11
$X_{1.5}BC$	33	0.21	26	−37.6	129 ± 9
$X_{2.0}BC$	28	0.19	27	−28.9	111 ± 10
$X_{2.5}BC$	25	0.14	22	−19.6	135 ± 20
$X_{0.5}AC$	36	0.26	29	−22.6	71 ± 5
$X_{1.0}AC$	58	0.30	21	−10.9	97 ± 10
$X_{1.5}AC$	27	0.15	22	−14.4	130 ± 5
$X_{2.0}AC$	33	0.25	30	−10.0	126 ± 10
$X_{2.5}AC$	23	0.12	20	−5.4	139 ± 11

[a] W: Without; X = MAF-OH; BC and AC: before and after calcination.

offered a broad peak centred at $2\Theta = 24°$, which suggests an amorphous feature of the samples (Fig. S5, ESI†).

The synthesised SiNPs exhibited a slight enhancement of the thermal stability due to the incorporation of HA, NA, PFPA, and PFHA, compared with those produced in the absence of such surfactants (Fig. S6, ESI†). The nitrogen adsorption and desorption isotherms indicated the formation of some porous structures using the aforementioned surfactants (Fig. S7 and Table S1, ESI†).

Almost identical functional and amorphous properties were observed with the use of MAF-OH before (BC) and after calcination (AC) as the above surfactants (Fig. S8–S13, ESI†). The FTIR spectra of the calcined samples displayed the disappearance of Si–OH and surfactant impurities, which indicates complete removal of the surfactant as well as further chemical condensation of hydroxyl functional groups in SiNPs at higher temperatures (Fig. S9, ESI†). Enhanced thermal stability was also encountered by the use of MAF-OH compared with the absence of MAF-OH (Fig. S12, ESI†). A slight change in thermal stability in the absence and presence of MAF-OH was attributed to an enhancement of SiNP density (the degradation behaviours of MAF-OH and other surfactants themselves are briefly described in the ESI with Fig. S12†). In the absence of the surfactant, a light opaque suspension was observed during the synthesis. In contrast, opaque milky white suspensions appeared due to the increase of the surfactant, which yielded denser SiNPs.

The nitrogen adsorption and desorption isotherms were also measured in the absence and presence of surfactant at various MAF-OH concentrations, BC and AC (Table 1, Fig. 5A and S13A, ESI†). The obtained results show that these materials also exhibited some porous structures. The surface area and pore volume values were decreased by the introduction of MAF-OH, regardless of the MAF-OH concentration. MAF-OH has hydrophilic carboxylic acid and hydroxyl functional group, and a hydrophobic fluorine functional group, which have strong interactions with the SiNPs. Such interactions produce dense particles, reducing the surface areas and pore volumes noticeably by increasing the surfactant concentration.[38] It is unclear, however, to observe such big differences with decreased surface area and pore volume in between when 1.0 mmol of MAF-OH was used to prepare SiNPs (BC) and when 0.5 mmol of the surfactant (BC) was used. Nevertheless, small differences with increased surface area and pore volume were noted for both different MAF-OH concentrations after calcination (AC). The slight changes in the pore volume before and after calcination might be due to the fact that the SiNPs do not have space enough for the accumulation and release of N_2 gas as well as due to the very low surface area and high density. At any rate, Table 1 as well as Fig. 5A and S13A† highlight the decreasing trend of the surface area and pore volume values when MAF-OH was introduced as a surfactant or for AC, although the trend was not consistent for all MAF-OH concentrations. The reproducibility was checked by two different experiments, which led to the same tendency.

It is also noted that the average pore diameter values were increased by an increase in the surfactant amount for BC, whereas no consistent trend was observed for AC (Fig. 5B and Table 1). A detailed investigation of the textural properties of the pores in the SiNPs prepared in the presence of MAF-OH is
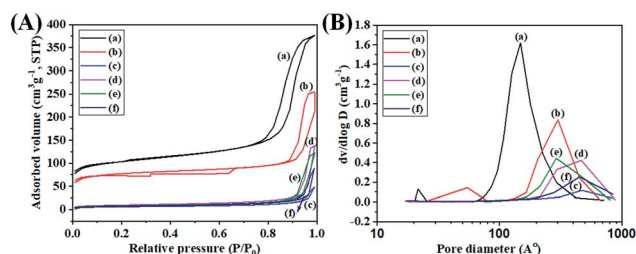

Fig. 5 (A) Nitrogen adsorption and desorption isotherms and (B) pore-size distribution curves of the SiNPs prepared (a) in the absence of MAF-OH, (b–f) in the presence of MAF-OH at various concentrations (0.5, 1.0, 1.5, 2.0, and 2.5 mmol), respectively, BC.

beyond the scope of this study. However, for convenience, 0.5 mmol of each surfactant, including MAF-OH, was used to prepare SiNPs to investigate the effects of different surfactants on the controlled synthesis of SiNPs. In addition, we focussed on the effect of MAF-OH concentrations on the shape and surface morphology of SiNPs, rather on the pore structures.

All samples BC and AC displayed negative zeta potential values (Table 1). Generally, SiNPs show positive or negative zeta potential values depending on pH conditions. The SiNPs become electrostatically stable when the values increase further to an extended level. SiNPs also exhibit more negative zeta potential values at mild acidic and basic conditions.[4,39,40] This leads to the formation of primary particles due to the nucleation of SiO_2 particles.[4,39,40] These results obey the isoelectric point of silica (pH $\sim$3).[41] The presence of both carboxylic and hydroxyl functional groups in MAF-OH slightly altered the pH of silica particles based on the MAF-OH amounts, which may be the reason to get some shift in the zeta potential values. In contrast, after calcination, the negative zeta potential values were reduced due to the removal of surface functional groups from the surfactant as well as the removal of excess of OH^- from the silica particles. Based on these reasons, we encountered some changes in the zeta potential values of the synthesised SiNPs with MAF-OH and other surfactants (Tables 1 and S1, ESI†).

The shape, surface morphology, and other properties of the SiNPs achieved from CTAB surfactant were also analysed using the same techniques (Fig. S14–S19, ESI†). The surface morphology of the SiNPs led to spheres with slight aggregation as well as higher particle size (approximately 780 ± 50 nm) BC and AC due to the long alkyl-chain compared with those of other surfactants (Fig. S14 and S15, ESI†). The particle size can be tuned under various experimental parameters, such as temperature, pH, concentrations of silane precursor and surfactant, rotation speed, and reaction time.

The synthesis of uniform and monodispersed nanoparticles depends upon the critical micelle concentration (CMC) of a surfactant because the CMC can control the micelle formation according to the concentration, pH, and temperature of the surfactant solution.[33,42,43] At a certain concentration, a surfactant can generate a micellar structure by self-assembly and form a uniform nanoparticle depending on the organic/inorganic compound. Banerjee *et al.*[33] determined the CMC of MAF-OH by fluoroscene spectroscopy using pyrene as a probe according to a reported procedure, and found its CMC value as around 2.3 mM.[33] In this work, a higher MAF-OH concentration than that of the CMC value, expecting the formation of unifrom and monodispersed nanoparticles by self-assembly of silane precursor on the micellar surface. Actually, the hydrophilic and hydrophobic functional groups in MAF-OH control the aggregation of particles and induce the formation of uniform monodispersed SiNPs. CTAB ($C_{19}H_{42}BrN$) can make a uniform cylindrical micelle at the concentration of 0.7 to 1.2 mM.[44,45] Furthermore, the synthesis of SiNPs was explored using CTAB (0.5 mmol) surfactant with a higher concentration than that of its CMC value. It should be noted that all other surfactants used in the study are anionic, while CTAB is cationic. CTAB is widely used as a structure-directing agent. Furthermore, it plays a vital

role in the synthesis of uniform SiNPs as well as mesoporous SiNPs based on the self-assembly, and also forms micelles in water. Hence, a further comparative experiment using CTAB was performed studying the roles of CTAB and other surfactants for the synthesis of uniform and monodispersed SiNPs. For a reference, the CMC values of HA, NA, PFPA, and PFHA were reported to be 1.4,[46] 50–70,[47] 51–82,[48,49] and 250 mM,[49] respectively.[46–49]

We found that MAF-OH and CTAB surfactants produced notable effects in the size- and morphology-controlled synthesis of SiNPs among such above tested surfactants. In addition, the CTAB produced SiNPs (780 ± 50 nm) with much larger sizes than those obtained involving MAF-OH. In contrast, HA, NA, PFPA, and PFHA produced uneven particle sizes with slight aggregation of SiNPs, which was due to the use of lower concentrations of NA, PFPA, and PFHA when comparing with their CMC values. Owing to this reason, the aforementioned surfactants can make some aggregations and form uneven nanoparticles. This behaviour is related to the delayed formation or even non-formation of complete micellar structure when the surfactant concentrations are lower than those of the CMC values of the surfactants.

The FTIR spectra of the synthesised SiNPs revealed strong C–H asymmetric and symmetric stretching frequencies at 2926 and 2854 cm^{-1} in addition to Si–O–Si, Si–OH, and C–C peaks, similar to other samples (Fig. S16a, ESI†). The peaks disappeared AC of the SiNPs, while strong Si–O–Si peaks appeared (Fig. S16b, ESI†). The samples also exhibited amorphous behaviour with considerably improved thermal stability than that of the sample produced in the presence of CTAB (Fig. S17 and S18, ESI†). These SiNPs also exhibited negative surface charges BC and AC. The CTAB-loaded SiNPs also demonstrated lower surface area (26 m^2 g^{-1}) and higher pore diameter values, whereas higher surface area (831 m^2 g^{-1}) and lower pore diameter (2.2 nm) values were obtained from the mesoporous structure by the calcination of the SiNPs (Fig. S19 and Table S1, ESI†).

Some other surfactants were also reported to prepare silica particles with different size, shape, morphology, and surface areas.[50–53] Typical anionic surfactants include sodium dodecyl sulfate (SDS), sodium oleate (SO), sodium dodecyl benzene sulfonate (SDBS). Cationic surfactants include dodecyltrimethylammonium bromide (DTAB), tetradecyltrimethylammonium bromide (TTAB), while non-ionic surfactants include Igepal CO-520 [polyoxyethylene (5) nonylphenylether, branched] and Brij 30 [polyoxyethylene(4) dodecyl ether, C12E4]. The use of SDS and SO anionic surfactants to prepare silica particles at $\sim$1 $\times$ 10^{-3} M concentration would increase the negative surface charge from −52 mV (for bare silica) to −68 and −66 mV, monodispersity, and particles sizes from 306 nm to 108–284 nm with photonic property.[50] In contrast, the introduction of CATB to prepare silica particles led to zeta potential of −38 mV with increased particles size (138 ± 33.6 nm), while the use of Igepal CO-520 non-ionic surfactant to prepare silica particles exhibited the zeta potential of $\sim$−53 mV and the particle size (107 ± 10.9 nm).[50] The homogeneity and mesoporous structure of silica particles were also reported to be

tuned by adding mixed anionic surfactants such as SDS and SDBS at certain concentrations.[51]

Conclusions

Several methods and approaches were reported to synthesise SiNPs in the presence or absence of a surfactant. Although various techniques were reported on uniform SiNPs in different approaches and conditions, in this work, however, for the first time, we have reported the use of an alternative surfactant., *i.e.* MAF-OH for the synthesis of uniform and monodispersed SiNPs. We carried out the synthesis at a particular experimental condition, and noted that without any surfactant, the particles were not quite uniform with some irregular particles size and shape. As a matter of fact, the introduction of MAF-OH can make more uniform and monodispersed SiNPs. Moreover, the size, shape, and dispersibility of the particles were also tuned by increasing the MAF-OH concentration at the same conditions. In order to compare the effect of MAF-OH surfactant on the synthesis of uniform SiNPs, we also used various other surfactants at a particular concentration and studied the size, shape, and morphology with various characterization tools. Unfortunately, other surfactants at particular concentration showed non-uniform morphology. Hence, we conclude that MAF-OH seems to behave as an alternative surfactant for uniform and size controlled synthesis of SiNPs in addition to the available methods. The surface area, pore volume, surface charge, and thermal stability of synthesised samples suggested that the SiNPs displayed lower surface area and pore volume, and negative surface charge with excellent thermal stability. The calcined SiNPs slightly altered above properties due to the complete removal of surfactant and the formation of denser particles by self-condensation at higher temperature. Our initial study supplies the idea to use the MAF-OH surfactant for the size controlled synthesis of various metal nanoparticles. In addition, the different surface properties and surface charges would suggest the possibility to use such SiNPs for diverse applications such as drug delivery, dye and metal adsorption, polymer nanocomposites, and coatings.

Conflicts of interest

There are no conflicts to declare.

Acknowledgements

References

1 P. G. Jeelani, P. Mulay, R. Venkat and C. Ramalingam, *Silicon*, 2020, **12**, 1337–1354.

2 A. Liberman, N. Mendez, W. C. Trogler and A. C. Kummel, *Surf. Sci. Rep.*, 2014, **69**, 132–158.

3 A. A. Vertegel, R. W. Siegel and J. S. Dordick, *Langmuir*, 2004, **20**, 6800–6807.

4 S. Nagappan, Y. Jeon, S. S. Park and C.-S. Ha, *ACS Omega*, 2019, **4**, 8548–8558.

5 S. Nagappan, H. M. Ha, S. S. Park, N.-J. Jo and C.-S. Ha, *RSC Adv.*, 2017, **7**, 19106–19116.

6 S. Nagappan, J. J. Park, S. S. Park, W.-K. Lee and C.-S. Ha, *J. Mater. Chem. A*, 2013, **1**, 6761–6769.

7 M. B. Gawande, Y. Monga, R. Zboril and R. K. Sharma, *Coord. Chem. Rev.*, 2015, **288**, 118–143.

8 I. Kim, A. J. Worthen, K. P. Johnston, D. A. DiCarlo and C. Huh, *J. Nanoparticle Res.*, 2016, **18**, 82.

9 Y. Wang, L. Zhang, Y. Hu and C. Li, *J. Mater. Sci. Technol.*, 2015, **31**, 901–906.

10 E. Rusen, A. Diacon, A. Mocanu, A. M. Dumitrescu and A. Dinescu, *Polym. Technol. Mater.*, 2020, **59**, 294–300.

11 D. Sriramulu, E. L. Reed, M. Annamalai, T. V. Venkatesan and S. Valiyaveettil, *Sci. Rep.*, 2016, **6**, 35993.

12 S. H. Wu and H. P. Lin, *Chem. Soc. Rev.*, 2013, **42**, 3862–3875.

13 M. Griffin, L. Nayyer, P. E. Butler, R. G. Palgrave, A. M. Seifalian and D. M. Kalaskar, *Nanomedicine Nanotechnology, Biol. Med.*, 2016, **12**, 1725–1733.

14 K. Tadanaga, K. Morita, K. Mori and M. Tatsumisago, *J. Sol-Gel Sci. Technol.*, 2013, **68**, 341–345.

15 I. A. Rahman and V. Padavettan, *J. Nanomater.*, 2012, **2012**, 132424.

16 C. Zhu, G. Zhao and W. Dou, *J. Sol-Gel Sci. Technol.*, 2018, **85**, 76–83.

17 E. D. Mohamed Isa, M. B. Abdul Rahman and H. Ahmad, *J. Porous Mater.*, 2018, **25**, 1439–1446.

18 M. C. Brochier Salon and M. N. Belgacem, *Colloids Surfaces A Physicochem. Eng. Asp.*, 2010, **366**, 147–154.

19 S. H. Wu, Y. Hung and C. Y. Mou, *Chem. Commun.*, 2011, **47**, 9972–9985.

20 M. W. Ambrogio, C. R. Thomas, Y. L. Zhao, J. I. Zink and J. F. Stoddart, *Acc. Chem. Res.*, 2011, **44**, 903–913.

21 X. Lv, L. Zhang, F. Xing and H. Lin, *Microporous Mesoporous Mater.*, 2016, **225**, 238–244.

22 Y. S. Chung, M. Y. Jeon and C. K. Kim, *Macromol. Res.*, 2009, **17**, 37–43.

23 T. G. Kim, G. S. An, J. S. Han, J. U. Hur, B. G. Park and S. C. Choi, *J. Korean Ceram. Soc.*, 2017, **54**, 49–54.

24 L. L. W. Wang and B. Gu, *J. Dispers. Sci. Technol.*, 2004, **25**, 593–601.

25 H. Yamada, C. Urata, S. Higashitamori, Y. Aoyama, Y. Yamauchi and K. Kuroda, *ACS Appl. Mater. Interfaces*, 2014, **6**, 3491–3500.

26 R. Narayan, U. Y. Nayak, A. M. Raichur and S. Garg, *Pharmaceutics*, 2018, **10**, 118.

27 J. W. Kim, L. U. Kim and C. K. Kim, *Biomacromolecules*, 2007, **8**, 215–222.

28 E. Murray, P. Born, A. Weber and T. Kraus, *Adv. Eng. Mater.*, 2010, **12**, 374–378.

29 B. Quan, C. Lee, J. S. Yoo and Y. Piao, *J. Mater. Chem. B*, 2017, **5**, 586–594.

30 Y. Han, Z. Lu, Z. Teng, J. Liang, Z. Guo, D. Wang, M. Y. Han and W. Yang, *Langmuir*, 2017, **23**, 5879–5890.

31 G. Ren, H. Su and S. Wang, *J. Sol-Gel Sci. Technol.*, 2020, **96**, 108–120.

32 S. Banerjee, T. Soulestin, Y. Patil, V. Ladmiral and B. Ameduri, *Polym. Chem.*, 2016, **7**, 4004–4015.

33 S. Banerjee, J. Schmidt, Y. Talmon, H. Hori, T. Asai and B. Ameduri, *Chem. Commun.*, 2018, **54**, 11399–11402.

34 F. Reis Da Cunha, I. Davidovich, Y. Talmon and B. Ameduri, *Polym. Chem.*, 2020, **11**, 2430–2440.

35 M. Yu, J. Yao, J. Liang, Z. Zeng, B. Cui, X. Zhao, C. Sun, Y. Wang, G. Liu and H. Cui, *RSC Adv.*, 2017, **7**, 11271–11280.

36 B. Bharti, J. Meissner, U. Gasser and G. H. Findenegg, *Soft Matter*, 2012, **8**, 6573–6581.

37 S. Yan, G. Zhinong, Y. Xia, X. Liao, J. Han, C. Pan, Y. Zhang and W. Zhai, *Eur. J. Inorg. Chem.*, 2018, **2018**, 1891–1901.

38 R. Filipović, Z. Obrenović, I. Stijepović, L. M. Nikolić and V. V. Srdić, *Ceram. Int.*, 2009, **35**, 3347–3353.

39 S. Wintzheimer, F. Miller, J. Prieschl, M. Retter and K. Mandel, *Nanoscale Adv*, 2019, **1**, 4277–4281.

40 G. F. Luo, W. H. Chen, Y. Liu, Q. Lei, R. X. Zhuo and X. Z. Zhang, *Sci. Rep.*, 2014, **4**, 6064.

41 R. Vacassy, R. J. Flatt, H. Hofmann, K. S. Choi and R. K. Singh, *J. Colloid Interface Sci.*, 2000, **227**, 302–315.

42 K. Kalyanasundaram and J. K. Thomas, *J. Am. Chem. Soc.*, 1977, **99**, 2039–2045.

43 L. Cai, M. Gochin and K. Liu, *Chem. Commun.*, 2011, **47**, 5527–5529.

44 M. A. Karimi, M. A. Mozaheb, A. Hatefi-Mehrjardi, H. Tavallali, A. M. Attaran and R. Shamsi, *J. Anal. Sci. Technol.*, 2015, **6**, 35.

45 S. Deodhar, P. Rohilla, M. Manivannan, S. P. Thampi and M. G. Basavaraj, *Langmuir*, 2020, **36**, 8100–8110.

46 D. Klostermeier and M. G. Rudolph, in *Biophysical Chemistry*, Taylor & Francis Group, 2018, p. 276.

47 R. Bomba, W. Kwiatkowski, A. Sánchez-Ferrer, R. Riek and J. Greenwald, *Biophys. J.*, 2018, **115**, 2336–2347.

48 K. Shinoda, T. Nakagawa, B.-I. Tamamushi and E. M. Loebl, in *Colloidal Surfactants: Some Physicochemical Propertie*, Academic Press, 1963, p. 53.

49 A. V. Alves, M. Tsianou and P. Alexandridis, *Surfaces*, 2020, **3**, 516–566.

50 W. Wang, B. Gu and L. Liang, *J. Colloid Interface Sci.*, 2007, **313**, 69–173.

51 F. Gai, T. Zhou, G. Chu, Y. Li, Y. Liu, Q. Huo and F. Akhtar, *Dalt. Trans.*, 2016, **45**, 508–514.

52 W. Wang, B. Gu and L. Liang, *J. Dispers. Sci. Technol.*, 2004, **25**, 593–601.

53 L. P. Singh, S. K. Bhattacharyya, G. Mishra and S. Ahalawat, *Appl. Nanosci.*, 2011, **1**, 117–122.